

# Quantized Anomalous Hall Insulator in a Nanopatterned Two-Dimensional Electron Gas

Yongping Zhang and Chuanwei Zhang\*

*Department of Physics and Astronomy, Washington State University, Pullman, WA, 99164 USA*

We propose that a quantum anomalous Hall insulator (QAHI) can be realized in a nanopatterned two-dimensional electron gas (2DEG) with a small in-plane magnetic field and a high carrier density. The Berry curvatures originating from the in-plane magnetic field and Rashba and Dresselhaus spin-orbit coupling, in combination with a nanoscale honeycomb lattice potential modulation, lead to topologically nontrivial insulating states in the 2DEG without Landau levels. In the bulk insulating gaps, the anomalous Hall conductivity is quantized  $-e^2/h$ , corresponding to a finite Chern number  $-1$ . There exists one gapless chiral edge state on each edge of a finite size 2DEG.

PACS numbers: 73.43.-f, 73.21.-b, 72.25.Dc, 72.20.-i

## I. INTRODUCTION

The quantum Hall effect was observed in a two-dimensional electron gas in the presence of a high perpendicular orbital magnetic field, which breaks the time reversal symmetry (TRS) and leads to Landau levels for quantum states. The TRS can also be broken spontaneously (*e.g.*, in a ferromagnetic phase) or by other means without the external orbital magnetic field and the associated Landau levels. The TRS breaking without Landau levels, together with spin-orbit coupling, yield the experimentally observed anomalous Hall effects (AHE) in ferromagnetic semiconductors<sup>1,2</sup>. The quantized version of the AHE, *i.e.*, a quantum anomalous Hall insulator (QAHI), is a band insulator with quantized charge Hall conductivity but without Landau levels. The QAHI was first proposed by Haldane in a honeycomb lattice with periodic magnetic fields that induce circulating current loops within one unit cell<sup>3,4</sup>. Motivated by the study of quantum spin Hall insulator<sup>5-11</sup>, the QAHI has been predicted recently to exist in HgMnTe quantum wells<sup>12</sup>, BiTe topological insulators<sup>13</sup>, and graphene with Rashba spin-orbit coupling<sup>14</sup>. In these proposals, the TRS is broken by an exchange Zeeman field induced by uniformly doping or adsorbing transition metal atoms. Schemes for realizing a QAHI using ultracold atoms in optical lattices<sup>15</sup> were also proposed. However, no experimental observation of the QAHI has been reported hitherto.

In this paper, we propose to realize a QAHI in a nanopatterned 2DEG with a high carrier density ( $\sim 10^{11}$  cm<sup>-2</sup>) and a small in-plane magnetic field ( $\sim 0.5$  T). The electrons in the 2DEG are modulated by an external nanoscale honeycomb lattice potential<sup>16</sup>, which has been experimentally realized in many solid state systems<sup>17-20</sup>. In our scheme, the required TRS breaking for the QAHI is achieved using a small in-plane magnetic field, which produces an in-plane Zeeman field for electrons. Note that an in-plane magnetic field does not induce orbital physics and the associated Landau levels. The 2DEG is confined in a semiconductor quantum well grown along the specific (110) direction<sup>21-23</sup> with both Rashba and Dresselhaus spin-orbit coupling. We show that a com-

ination of the honeycomb lattice modulation, Rashba and Dresselhaus spin-orbit coupling, and the small in-plane magnetic field, can open two topologically nontrivial bulk energy gaps in the spectrum, in which the charge Hall conductivity is quantized  $-e^2/h$  (corresponds to a finite Chern number  $-1$ ). Here  $e$  is the charge of electron and  $h$  is the Plank constant. We calculate the Berry curvature distribution and characterize the dependence of the anomalous Hall conductivity on the chemical potential. We show that there exist one gapless chiral edge state on each edge of a finite size 2DEG, consisting with the Chern number  $-1$ . Finally, we show that the QAHI can be observed in a wide range of experimentally feasible parameters.

There are two main advantages of using the nanopatterned 2DEG for realizing a QAHI: 1) The 2DEG has been studied for several decades and accumulated technology for semiconductors makes it a promising experimental candidate. One outstanding feature of a 2DEG is its high purity, leading to high mobility of electrons. 2) The small in-plane magnetic field ( $\sim 0.5$ T) can be generated using permanent bar magnets or magnetic current coils, which are much easier to implement and tune to a large magnitude in experiments than doping or adsorbing transition metal elements in topological insulator or graphene<sup>12-14</sup>. The bar magnets or coils can be easily integrated into the design of the QAHI, and their great tunability (compared to doping magnetic atoms) may lead to new functionality for device applications.

The paper is organized as follows: Section II illustrates the proposed experimental setup for the observation of QAHI. Section III describes the QAHI in a 2DEG in the presence of a honeycomb lattice potential modulation and an in-plane magnetic field. The experimental parameters for the observation of the QAHI is also discussed. Section IV is the conclusion.

## II. PROPOSED EXPERIMENTAL SCHEME

The proposed experimental scheme is illustrated in Fig. 1. A 2DEG is confined in a quantum well grown

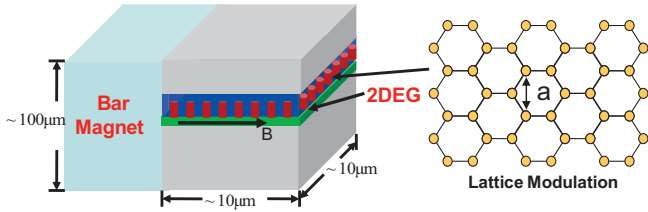


FIG. 1. (Color online) Schematic illustration of the proposed experimental scheme. The 2DEG confined in a quantum well grown along (110) direction, which possesses Rashba and Dresselhaus spin-orbit coupling simultaneously. A small in-plane magnetic field, generated by bar magnets or magnetic current coils, is applied to generate an in-plane Zeeman field. There are nanoscale periodic modulation pillars (radius  $b$ ) with a honeycomb lattice structure on top of the 2DEG.

along the (110) direction<sup>21,22</sup> with the layer inversion symmetry explicitly broken by imbalancing the quantum well using a gate voltage and/or chemical means. The Rashba and Dresselhaus spin-orbit coupling coexist in such a 2DEG, and the dynamics of electrons in the presence of an in-plane magnetic field can be described by the Hamiltonian<sup>23</sup>,

$$H_0 = \frac{\hbar^2 k^2}{2m^*} + \alpha_R(k_y \sigma_x - k_x \sigma_y) + \alpha_D k_x \sigma_z + h_y \sigma_y, \quad (1)$$

where  $m^*$  is the effective mass of electrons in the conduction band,  $\alpha_R$  and  $\alpha_D$  are the strengths of Rashba and Dresselhaus spin-orbit coupling respectively,  $\hat{\sigma} = (\sigma_x, \sigma_y, \sigma_z)$  are Pauli matrices, and  $h_y$  is the magnitude of the in-plane Zeeman field induced by a small in-plane magnetic field that can be generated by bar magnets or magnetic current coils. The Hamiltonian (1) has two eigenenergies  $E_{\pm\mathbf{k}} = \frac{\hbar^2 k^2}{2m^*} \pm E_0$  with

$$E_0 = \sqrt{\alpha_D^2 k_x^2 + \alpha_R^2 k_y^2 + (\alpha_R k_x - h_y)^2}. \quad (2)$$

The minimum energy gap between two bands is  $\Delta = 2\alpha_D h_y / \sqrt{\alpha_D^2 + \alpha_R^2}$  that occurs at  $k_x = \alpha_R h_y / (\alpha_D^2 + \alpha_R^2)$  and  $k_y = 0$ . The gap is nonzero only for nonzero  $\alpha_D$  and  $h_y$ . The 2DEG is modulated by a two-dimensional honeycomb lattice potential (Fig. 1)

$$V(\mathbf{r}) = V_0 \text{ if } |\mathbf{r} - \mathbf{r}_j| \leq b; \text{ otherwise } 0, \quad (3)$$

where  $\mathbf{r}_j$  is the honeycomb lattice point,  $b$  is the radius of the nanoscale pillar, and the lattice constant  $a_0 = a/\sqrt{3}$ . The lattice structure has been realized in a GaAs 2DEG in a recent experiment<sup>17,18</sup>.

### III. QAHI IN A 2DEG

#### A. 2DEG without lattice modulation

Before presenting the QAHI physics with the lattice modulation, we first discuss the intrinsic AHE in

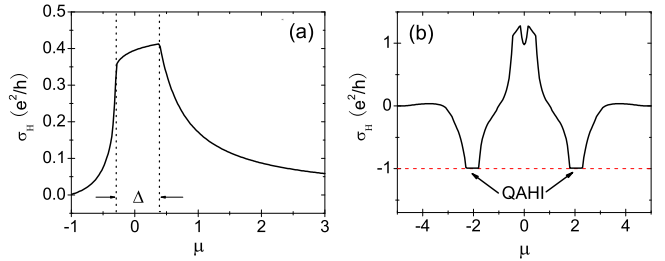


FIG. 2. Plot of the anomalous charge Hall conductivity  $\sigma_H$  versus the chemical potential  $\mu$  without (a) or with (b) lattice modulation. (a)  $\alpha_D k_c = 0.8$ ,  $\alpha_R k_c = 0.8$ ,  $h_y = 0.5$ . The space between dashed lines is the gap  $\Delta$  between two energy bands. The energy unit is chosen as  $\hbar^2 k_c^2 / m^*$ , with  $k_c = 3 \text{ nm}^{-1}$  for  $\alpha_D = 0.3 \text{ eV}\cdot\text{\AA}$ . (b)  $\lambda_R = 0.3$ ,  $\lambda_D = 0.8$ ,  $h_y = 1.6$ . The energy unit is tunneling amplitude  $t$ .

the 2DEG without the lattice potential, which originate from the nontrivial topological properties induced by the spin-orbit coupling and the in-plane Zeeman field. The Rashba and Dresselhaus spin-orbit coupling, together with the TRS breaking induced by the in-plane Zeeman field, yield non-zero Berry curvatures  $\Omega_{\pm} = -2\text{Im}\langle \frac{\partial \Phi_{\pm}}{\partial k_x} | \frac{\partial \Phi_{\pm}}{\partial k_y} \rangle \mathbf{e}_z$  for electrons in the two energy bands  $E_{\pm\mathbf{k}}$ . Here  $\Phi_{\pm}$  are the eigenfunctions of the Hamiltonian (1).

Straightforward calculation shows

$$\Omega_{\pm} = \mp \alpha_R \alpha_D h_y \mathbf{e}_z / 2E_0^3, \quad (4)$$

which have the same amplitude but opposite sign in two bands.  $\Omega_{\pm}$  are equivalent to an effective magnetic field in momentum space and yield an anomalous velocity of electrons  $\mathbf{v} = e\mathbf{E} \times \Omega_{\pm}$  when an electric field  $\mathbf{E}$  is applied<sup>2</sup>. The intrinsic AHE is the manifestation of the anomalous velocity of electrons with the Hall conductivity

$$\sigma_H = \frac{e^2}{h} \sum_n \int \frac{dk_x dk_y}{2\pi} \Omega_n f(E_{n\mathbf{k}}), \quad (5)$$

where  $f(E_{n\mathbf{k}}) = 1 / (e^{(E_{n\mathbf{k}} - \mu) / k_B T} + 1)$  is the Fermi-Dirac distribution,  $\mu$  the chemical potential,  $n = \pm$  is the band index,  $k_B$  is the Boltzmann constant and  $T$  is the temperature.

Fig. 2a shows the dependence of  $\sigma_H$  on the chemical potential  $\mu$  at zero temperature.  $\mu$  can be tuned in experiments by varying the gate voltage of the quantum well. When  $\mu$  lies just above the energy minimum of the lower band, the Berry curvature for occupied electrons is small and  $\sigma_H$  is small. When  $\mu$  sweeps across the energy gap between two bands,  $\sigma_H$  reaches the maximum. Further increase of  $\mu$  leads to the occupation of electrons in the upper band and the decrease of  $\sigma_H$  due to the cancellation of the contributions from two bands with opposite sign of the Berry curvatures. When  $\mu \rightarrow \infty$ , the total  $\sigma_H$  approaches zero.

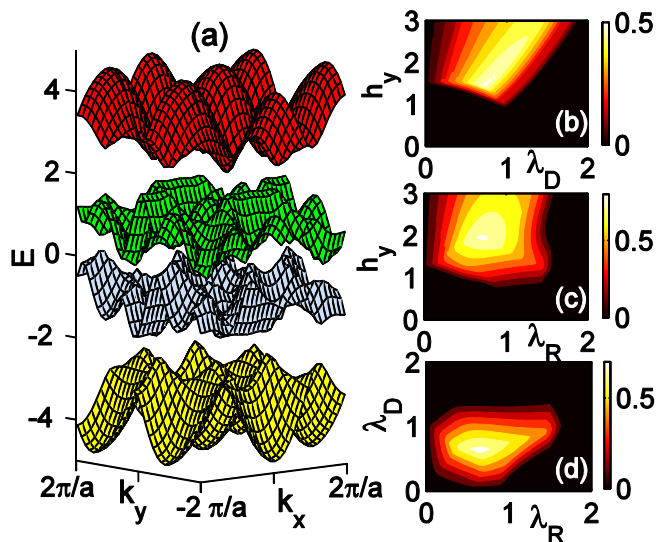


FIG. 3. (Color online) (a) Plot of the energy spectrum of the tight-binding Hamiltonian (6).  $\lambda_R = 0.3$ ,  $\lambda_D = 0.8$  and  $h_y = 1.6$ . (b)-(d) Plot of the bulk energy gap between the lowest two bands for different parameters. (b)  $\lambda_R = 0.3$ . (c)  $\lambda_D = 0.8$ . (d)  $h_y = 1.5$ .

### B. QAHI with lattice modulation

A QAHI is a band insulator with a bulk energy gap opened in the spectrum. Generally, a bulk energy gap can be obtained by coupling electrons to a periodic lattice potential, which transforms the plane wave states to the Bloch states of electrons. In this Letter, we consider a honeycomb lattice potential modulation (3) of the 2DEG in the tight-binding region, where the free space Hamiltonian (1) changes to

$$H = -t \sum_{\langle ij \rangle} c_i^\dagger c_j + i\lambda_R \sum_{\langle ij \rangle} c_i^\dagger [\hat{\sigma} \times \mathbf{d}_{ij} \cdot \mathbf{e}_z] c_j + i\lambda_D \sum_{\langle ij \rangle} c_i^\dagger [\hat{\sigma} \times \mathbf{d}_{ij} \cdot \mathbf{e}_y] c_j + h_y \sum_i c_i^\dagger \sigma_y c_i, \quad (6)$$

where  $c_i^\dagger (c_i)$  creates (annihilates) an electron at site  $i$ ,  $\langle ij \rangle$  represents two nearest neighboring sites,  $t = \int d^2\mathbf{r} \Phi^*(\mathbf{r}) V(\mathbf{r}) \Phi(\mathbf{r} - \mathbf{a})$  is the spin-independent nearest neighbor tunneling strength,  $\Phi(\mathbf{r})$  is the eigenstates of a single pillar centered at the origin and  $\mathbf{a}$  is a nearest-neighbor position vector. For  $b/a_0 \sim 0.23$ ,  $t/E_L \sim 0.06 \exp(-V_0/0.85E_L)^{17,18}$ , where  $E_L = \frac{\hbar^2}{2m^*} \left(\frac{2\pi}{a_0}\right)^2$  is the energy defined by the lattice constant  $a_0$ .  $\lambda_R$  and  $\lambda_D$  are the spin-dependent nearest neighbor tunneling strengths originating from Rashba and Dresselhaus spin-orbit coupling,  $\mathbf{d}_{ij}$  is the unit bond vector between nearest neighboring sites  $i$  and  $j$ ,  $h_y$  is the in-plane Zeeman field. Henceforth we set  $t = 1$  as the energy unit.

The energy spectrum is obtained by numerically diagonalizing the tight-binding Hamiltonian (6) in momentum space through the Fourier transformation  $c_i(\tau, \sigma) =$

$\sum_{\mathbf{k}} c_{\mathbf{k}}(\tau, \sigma) \exp(-i\mathbf{k} \cdot \mathbf{R}_i)$ , assuming a periodic boundary condition of the system. Here  $\tau = \{A, B\}$  represent two sublattice degrees of freedom of electrons in a honeycomb lattice, and  $\sigma = \{\uparrow, \downarrow\}$  are the spin degrees of freedom. These four degrees of freedom lead to four energy bands of the Hamiltonian (6), as plotted in Fig. 3a. There are energy gaps opened between the lowest two bands and the highest two bands respectively. The gaps exist for a wide range of physical parameters. Taking account of the symmetry between two gaps, we only need characterize the gap between the lowest two bands, which is plotted in Figs. 3b-3d for different parameters. Figs. 3b and 3c have constant  $\lambda_R = 0.3$  and  $\lambda_D = 0.8$  respectively. Clearly, the gap is opened only above a critical value of  $h_y$ . Fig. 3d is plotted with a fixed  $h_y = 1.5$ . The gap only exists in certain area in the parameter plane spanned by  $\lambda_R$  and  $\lambda_D$ . The presence of the bulk energy gap indicates an insulating state of the system. Another interesting feature of our system is that there is no gap between the second and third bands. Instead, the valley centers at these two bands shift to opposite directions due to the lack of in-plane rotation symmetry of the Hamiltonian (6). Although these two bands do not touch at any  $\mathbf{k}$ , a full energy gap does not exist. This is very different from the graphene scheme with Rashba spin-orbit coupling and perpendicular exchange field, where the gap is opened between the second and third bands<sup>14</sup>.

The nanopatterned 2DEG inherits the topological properties of the 2DEG without the lattice modulation. We numerically calculate the Berry curvature distribution in the lowest band and plot it in Fig. 4. The peaks of the Berry curvatures shift toward the positive  $k_x$  direction from the corners of the Brillouin zone, which can be understood from the fact that the Berry curvature (4) without the lattice modulation has a peak at  $k_x = \alpha_R h_y / (\alpha_D^2 + \alpha_R^2)$  due to the in-plane Zeeman field and Dresselhaus spin-orbit coupling that destroy the rotation symmetry in the plane.

When the chemical potential lies inside the bulk gap, the 2DEG is an insulator and there is no longitudinal current with an applied electric field. However, as we have

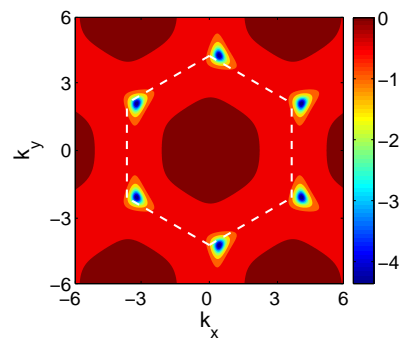


FIG. 4. (Color online) Contour plot of the Berry curvature in the lowest band.  $\lambda_R = 0.3$ ,  $\lambda_D = 0.8$ ,  $h_y = 1.6$ . The dashed line is the boundary of the first Brillouin zone of the honeycomb lattice.

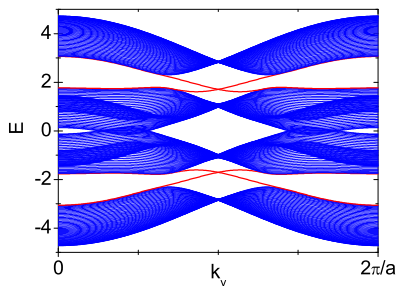


FIG. 5. (Color online) Band spectrum of a nanopatterned 2DEG with a zigzag boundary along the  $x$  direction.  $\lambda_R = 0.3$ ,  $\lambda_D = 0.8$ ,  $h_y = 1.6$ . The red lines are the gapless chiral edge states.

discussed in the case without lattice modulation, the non-zero Berry curvature can yield a transversal Hall current by inducing an anomalous velocity of electrons. The anomalous Hall conductivity  $\sigma_H$ , calculated from Eq. (5) by integrating the Berry curvature over the first Brillouin zone, is found to be quantized  $-e^2/h$  in both gaps (Fig. 2b). The quantized  $\sigma_H$  is directly related to the topological invariant of the system known as the first Chern number  $\mathcal{C}^{24}$ . The Hall conductivity can be expressed as  $\sigma_H = \frac{e^2}{h}\mathcal{C}$ , with

$$\mathcal{C} = \int_{BZ} \frac{d^2k}{2\pi} \Omega \quad (7)$$

as the integral over the first Brillouin zone. Therefore  $\mathcal{C} = -1$  for both gaps in the nanopatterned 2DEG. Note that here the quantized anomalous Hall conductivity originates from the interplay between the sublattice and spin degrees of freedom of electrons in the honeycomb lattice. We have checked that a simple square lattice modulation does not lead to the quantized  $\sigma_H$ .

In a QAHI, currents flowing along the boundary of the system form gapless chiral edge states within the gap, which are the manifestation of the quantized Hall conductivity obtained from the bulk topological property. The emergence of gapless chiral edge states can be obtained from the energy spectrum of a finite two dimensional system. We construct a finite size nanopatterned 2DEG that has a zigzag boundary along the  $x$  direction and is infinite along the  $y$  direction. The resulting energy spectrum is shown in Fig. 5. There are still two gaps opened between the lowest two bands and the highest two bands. Within each gap, there exist two gapless chiral edge states on two edges of this finite size 2DEG. The number of edge states on each edge is equal to the absolute value of the first Chern number  $|\mathcal{C}| = 1$ , as expected. The chiral edge currents can be probed in a typical six-probe Hall-bar experimental setup.

### C. Experimental parameters

In experiments, the honeycomb potential modulation on a 2DEG with a typical lattice constant  $a_0 \sim 130$

nm has been realized<sup>17,18</sup>. More generally, nanostructures with the square lattice geometry and a typical lattice constant  $a_0 \sim 10$  nm have also been realized in many experiments<sup>19,20</sup>. Implementing honeycomb lattice structures with similar small lattice constants should be straightforward. We consider InSb semiconductor quantum wells with large spin-orbit coupling. The effective mass of electrons in the conduction bands is  $m^* = 0.014m_e$ , therefore the corresponding energy unit of the lattice system is  $E_L = \frac{\hbar^2}{2m^*} \left(\frac{2\pi}{a_0}\right)^2 \sim 6.2$  meV for  $a_0 \sim 130$  nm, and  $b \sim 30$  nm. For a lattice depth  $V_0 = 0.6E_L \sim 3.7$  meV and electron density  $n \sim 5 \times 10^9$  cm<sup>-2</sup> (roughly one electron per site), the nanopatterned 2DEG is in the tight-binding region, with a typical tunneling strength between neighboring lattice sites  $t \sim 0.03E_L \sim 0.2$  meV. For  $a_0 \sim 130$  nm, the typical Rashba and Dresselhaus spin-orbit coupling strength that can be reached in an InSb 2DEG are  $\lambda_R \sim 0.08$  meV, and  $\lambda_D \sim 0.2$  meV<sup>23</sup>, which are within the parameter region where the band gaps are opened. The InSb also has a large  $g$  factor  $g \sim 70$ <sup>25</sup>, which ensures an in-plane Zeeman energy  $h_y \sim 0.25$  meV can be easily realized with a small magnetic field  $\sim 0.1$  T generated by bar magnets or magnetic current coils. The resulting gap size is  $\sim 0.15$  meV, which corresponds to  $\sim 2$  K temperature and can be easily achieved in a 2DEG.

The size of the gap and the density of electrons can be further increased by using a smaller lattice constant in experiments. For instance, for  $a_0 \sim 30$  nm,  $b \sim 7$  nm with corresponding spin-orbit coupling energies  $\lambda_R \sim 0.35$  meV,  $\lambda_D \sim 0.8$  meV, a set of physical parameters within current experimental technology are  $E_L \sim 116$  meV,  $B \sim 0.5$  T,  $h_y \sim 1$  meV,  $n \sim 1.3 \times 10^{11}$  cm<sup>-2</sup>, and  $t \sim 0.008E_L \sim 0.8$  meV for  $V_0 \sim 1.8E_L$ . The resulting gap is now  $\sim 0.5$  meV ( $\sim 6$  K). With such a high carrier density  $n$  and the high mobility of electrons in the 2DEG<sup>26</sup>, the effects of disorder can be neglected<sup>18,26</sup>. To reduce the required magnitude of  $V_0$ , a two-dimensional hole gas may be used, which has larger effective mass  $m_h^* = 0.43m_e$ , leading to much smaller  $E_L^h = 0.03E_L$ . Finally, we remark that although quantum Hall effects have been observed in graphene at a medium magnetic field  $\sim 2$  T<sup>27</sup>, the Hall plateau is small and the corresponding Hall conductivity  $\sigma_H = 14e^2/h$  (a very large magnetic field ( $> 10$  T) is needed to reach  $\sigma_H = e^2/h$ ).

## IV. CONCLUSION

In summary, we find that a QAHI can be realized in a 2DEG with a high carrier density, a small magnetic field, and a nanoscale honeycomb lattice potential modulation. We show that topologically nontrivial band energy gaps can be opened, within a wide range of experimentally feasible parameters, through a combination of the honeycomb lattice, Rashba and Dresselhaus spin-orbit coupling, and a small in-plane magnetic field. Quantum

anomalous Hall effects can be observed in the bulk gaps with a quantized Hall conductivity  $\sigma_H = -e^2/h$ , corresponding to a Chern number  $C = -1$ .

**Acknowledgement:** We thank Vito Scarola for valuable discussion. This work is supported by

ARO (W911NF-09-1-0248), DARPA-MTO (FA9550-10-1-0497), and DARPA-YFA (N66001-10-1-4025). Y.Z. is also supported by DOE (DE-FG02-02ER45958, Division of Materials Science and Engineering) and Welch Foundation (F-1255).

---

\* cwzhang@wsu.edu

- <sup>1</sup> N. Nagaosa, J. Sinova, S. Onoda, A. H. MacDonald, and N. P. Ong, *Rev. Mod. Phys.* **82**, 1539 (2010)
- <sup>2</sup> D. Xiao, M.-C. Chang, and Q. Niu, *Rev. Mod. Phys.* **82**, 1959 (2010).
- <sup>3</sup> F. D. M. Haldane, *Phys. Rev. Lett.* **61**, 2015 (1988).
- <sup>4</sup> M. Onoda and N. Nagaosa, *Phys. Rev. Lett.* **90**, 206601 (2003).
- <sup>5</sup> B. A. Bernevig, T. L. Hughes, and S.-C. Zhang, *Science* **314**, 1757 (2006).
- <sup>6</sup> C. L. Kane, and E. J. Mele, *Phys. Rev. Lett.* **95**, 226801 (2005).
- <sup>7</sup> L. Fu, C. Kane, and E. J. Mele, *Phys. Rev. Lett.* **98**, 106803 (2007).
- <sup>8</sup> X.-L. Qi, T. L. Hughes, and S.-C. Zhang, *Nat. Phys.* **4**, 273 (2008).
- <sup>9</sup> J. E. Moore, *Nat. Phys.* **5**, 378 (2009).
- <sup>10</sup> M. Z. Hasan, and C. L. Kane, *Rev. Mod. Phys.* **82**, 3045 (2010).
- <sup>11</sup> X.-L. Qi, and S.-C. Zhang, arXiv:1008.2026.
- <sup>12</sup> C.-X. Liu, X.-L. Qi, X. Dai, Z. Fang, and S.-C. Zhang, *Phys. Rev. Lett.* **101**, 146802 (2008).
- <sup>13</sup> R. Yu, W. Zhang, H.-J. Zhang, S.-C. Zhang, X. Dai, and Z. Fang, *Science* **329**, 61 (2010).
- <sup>14</sup> Z. Qiao, S. A. Yang, W. Feng, W.-K. Tse, J. Ding, Y. Yao, J. Wang, and Q. Niu, *Phys. Rev. B* **82**, 161414 (2010).
- <sup>15</sup> C. Wu, *Phys. Rev. Lett.* **101**, 186807 (2008).
- <sup>16</sup> C.-H. Park and S. G. Louie, *Nano Lett.* **9**, 1793 (2009).
- <sup>17</sup> M. Gibertini, A. Singha, V. Pellegrini, and M. Polini, *Phys. Rev. B* **79**, 241406 (R) (2009).
- <sup>18</sup> G. F. Simoni, A. Singha, M. Gibertini, B. Karmakar, M. Polini, V. Piazza, L. N. Pfeiffer, K. W. West, F. Beltram, and V. Pellegrini, *App. Phys. Lett.* **97**, 132113 (2010).
- <sup>19</sup> S.Y. Chou, P. R. Krauss, W. Zhang, L. Guo, and L. Zhuang, *J. Vac. Sci. Technol. B* **15**, 2897 (1997).
- <sup>20</sup> W. F. van Dorp, B. v. Someren, C. W. Hagen, and P. Kruit, *Nano Lett.* **5**, 1303 (2005).
- <sup>21</sup> Y. Ohno, R. Terauchi, T. Adachi, F. Matsukura, and H. Ohno, *Phys. Rev. Lett.* **83**, 4196 (1999).
- <sup>22</sup> V. Sih, R. C. Myers, Y. K. Kato, W. H. Lau, A. C. Gossard and D. D. Awschalom, *Nat. Phys.* **1**, 31 (2005).
- <sup>23</sup> J. Alicea, *Phys. Rev. B* **81**, 125318 (2010).
- <sup>24</sup> D. J. Thouless, M. Kohmoto, M. P. Nightingale, and M. den Nijs, *Phys. Rev. Lett.* **49**, 405 (1982).
- <sup>25</sup> H. A. Nilsson, *Nano Lett.* **9**, 3151 (2009).
- <sup>26</sup> K.J. Goldammer, S. J. Chung, W. K. Liu, and M. B. Santos, *J. Crystals Growth* **201**, 753 (1999).
- <sup>27</sup> J. Jiang, Y. Zhang, Y.-W. Tan, H.L. Stormer, and P. Kim, *Solid Stat. Comm.* **143**, 14 (2007).